RADAR CROSS SECTION OF UNDERDENSE TURBULENT WAKES

Ronald L. Fante

Air Force Cambridge Research Laboratories
L. G. Hanscom Field, Massachusetts

11 October 1973

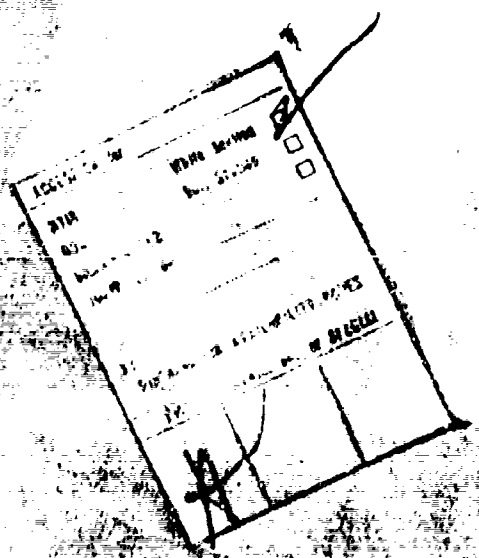

Unclassified
Security Classification

AD 775 083

DOCUMENT CONTROL DATA - R&D

(Security classification of title, body of abstract and indexing annotation must be entered when the overall report is classified)

1. ORIGINATING ACTIVITY *(Corporate author)*
Air Force Cambridge Research Laboratories (LZP)
L. G. Hanscom Field
Bedford, Massachusetts 01730

2a. REPORT SECURITY CLASSIFICATION
Unclassified

2b. GROUP

3. REPORT TITLE

RADAR CROSS SECTION OF UNDERDENSE TURBULENT WAKES

4. DESCRIPTIVE NOTES *(Type of report and inclusive dates)*
Scientific. Interim.

5. AUTHOR(S) *(First name, middle initial, last name)*

Ronald L. Fante

6. REPORT DATE	7a. TOTAL NO. OF PAGES	7b. NO. OF REFS
11 October 1973	14	7

8a. CONTRACT OR GRANT NO.	9a. ORIGINATOR'S REPORT NUMBER(S)
b. PROJECT, TASK, WORK UNIT NOS. 56350401	AFCRL-TR-73-0634
c. DOD ELEMENT 61102F	9b. OTHER REPORT NO(S) *(Any other numbers that may be assigned this report)*
d. DOD SUBELEMENT 681305	PSRP No. 568

10. DISTRIBUTION STATEMENT

Approved for public release; distribution unlimited.

11. SUPPLEMENTARY NOTES	12. SPONSORING MILITARY ACTIVITY
TECH, OTHER	Air Force Cambridge Research Laboratories (LZP) L. G. Hanscom Field Bedford, Massachusetts 01730

13. ABSTRACT

Using transport theory, we have calculated the radar cross section of an underdense turbulent wake in the limit when the scale size of the turbulence is larger than the signal wavelength. We have found that for bistatic scatter the first Born approximation is valid, even if the wake is many photon mean-free paths in extent. However, neither the Born approximation nor the modified Born approximation is valid for the monostatic radar cross section when the wake is many photon mean-free paths in extent. In this case a modified result, derived in this report, must be used.

DD FORM 1 NOV 68 1473

Unclassified
Security Classification

14. KEY WORDS	LINK A		LINK B		LINK C	
	ROLE	WT	ROLE	WT	ROLE	WT
Turbulent plasma						
Radar cross section						
Wake radar cross section						
Underdense plasma						

Contents

1. INTRODUCTION	5
2. ANALYSIS	6
3. CALCULATIONS OF THE RCS	12
4. AN EXAMPLE	12
5. CONCLUSIONS	14
REFERENCES	15

Illustrations

1. Assumed Geometry for the Derivation of the Scattered Intensity	6
2. Geometry Assumed in the Derivation of Eqs. (19)-(21)	11
3. Model Used to Relate the Scattered Intensity to the RCS	12
4. Scattering by a Turbulent Parallelepiped	13

Radar Cross Section of Underdense Turbulent Wakes

I. INTRODUCTION

There has been considerable interest in the radar cross section (RCS) of the turbulent wake of a reentry vehicle. Generally, this has been calculated using the Born approximation[1-3] or a modified Born approximation[4], and the above calculation is valid when the dimension of the wake in the propagation direction is less than the mean free path for photon scatter. This is an acceptable approximation for the RCS of a short underdense wake. However, for longer wakes the Born approximation is no longer accurate, and more exact techniques must be employed to calculate the RCS. In this report we will employ transport theory to obtain an exact expression for the RCS of an underdense turbulent plasma in which the dimensions of the plasma are large compared with the photon mean-free path.

(Received for publication 10 October 1973)

1. Booker, H. (1959) Radio scattering in the lower ionosphere, J. Geophys. Res. 64:2164-2177.
2. Salpeter, E., and Trieman, S. (1954) Backscatter of electromagnetic radiation from turbulent plasma, J. Geophys. Res. 69:869-881.
3. Luzzi, T. E. (1969) EM scattering from a finite volume turbulent plasma, IEEE Trans. Antenna & Propagation AP-17:342-348.
4. Graf, K. A., and Guthart, H. (1971) Application of a simple model for calculating scatter, Phys. Fluids 14:410-413.

2. ANALYSIS

To study the scattering from an underdense turbulent plasma we consider the model shown in Figure 1. We assume that the incident field is a plane wave propagating along the z-axis, and that the receiver is located in the backward hemisphere

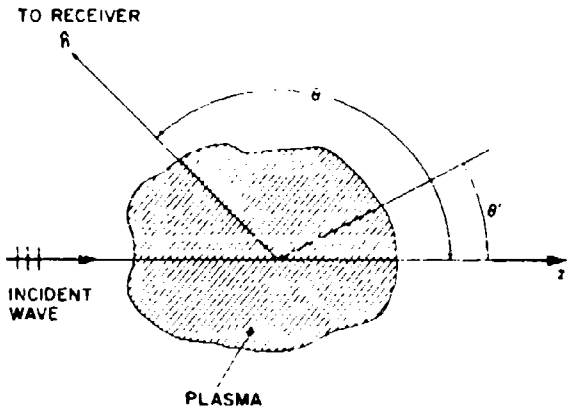

Figure 1. Assumed Geometry for the Derivation of the Scattered Intensity

($\pi/2 < \theta \leq \pi$), and lies in the Fraunhofer zone of the plasma. We further assume that: (1) the plasma is underdense, (2) the scale size L of the turbulence is such that $k_0 L >> 1$, where k_0 is the wavenumber of the incident signal, (3) the scale size L of the turbulence is much less than the mean free path, ℓ_s, for photon scatter. When these assumptions hold, it can be shown[5] that the ensemble averaged radiative intensity $I(\underline{x}, \hat{n})$ in the direction of the unit vector $\hat{n}$ satisfies

$$\left(\hat{n} \cdot \nabla + \frac{1}{\ell}\right) I(\underline{x}, \hat{n}) = \iint d\Omega' \sigma_s(\hat{n}, \hat{n}') I(n') . \tag{1}$$

In Eq. (1), $d\Omega$ is the element of solid angle,

$$\frac{1}{\ell} = \frac{1}{\ell_s} + \frac{1}{\ell_a} , \tag{2}$$

5. Watson, K. M. (1969) Multiple scattering of electromagnetic waves in a dense plasma, J. Math. Phys. 10:688-702.

$$\frac{1}{\ell_a} = \left(\frac{\nu_c}{c}\right) \frac{\omega_p^2}{\omega_p^2 + \nu_c^2} , \tag{3}$$

where ω_p is the electron plasma frequency, ν_c is the electron-neutral collision frequency, and c is the speed of light. The quantity σ_g is the scattering cross section per unit volume, and is given by

$$\sigma_g = \frac{r_o^2 n_e^2 (x)}{\left(1 + \frac{\nu_c^2}{\omega_p^2}\right)} \iiint d^3 r\, g(\underline{x}, \underline{r}) \exp\left[i k_o \rho_1 (\hat{n} - \hat{n}') \cdot \underline{r}\right], \tag{4}$$

where r_o is the classical electron radius, n_e is the ensemble averaged electron density, $g(x, r)$ is the pair correlation function and $\rho_1 = 1 - \omega_p^2/(\omega^2 + \nu_c^2)$. Finally, the mean-free path, ℓ_t, for photon scatter is given by

$$\frac{1}{\ell_t} = \frac{1}{2} \iint d\Omega' \sigma_g (\hat{n}, \hat{n}') \left(1 + \cos^2 \theta_s\right), \tag{5}$$

where θ_s is the angle between $\hat{n}$ and $\hat{n}'$.

We now consider Eq. (1) for the case when $\hat{n}$ lies in the backward hemisphere, and we rewrite Eq. (1) as

$$\left(\hat{n} \cdot \nabla + \frac{1}{\ell}\right) I(\hat{n}) = \iint_{\Omega_+} d\Omega' \sigma_g (\hat{n}, \hat{n}') I(\hat{n}') + \iint_{\Omega_-} d\Omega \sigma_g (\hat{n}, \hat{n}') I(\hat{n}') , \tag{6}$$

where Ω_+ is the forward hemisphere and Ω_- is the backward hemisphere. Now when $k_o L >> 1$, it can be shown that in the forward hemisphere $I(\hat{n})$ is sharply peaked about $\theta = 0$. Therefore, in the first integral on the right hand side of Eq. (6), σ_g may be expanded in Taylor series about $\theta' = 0$ to give

$$\sigma_g(\theta, \theta') = \sigma_g(\theta) + \theta' \left[\frac{\partial \sigma_g(\theta, \theta')}{\partial \theta}\right]_{\theta' = 0} + \frac{(\theta')^2}{2} \left[\frac{\partial^2 \sigma_g(\theta, \theta')}{\partial \theta'^2}\right]_{\theta' = 0} + \ldots .$$

Upon using this expression in the first term on the right hand side of Eq. (6), we get

$$\iint_{\hat{\Omega}'_+} d\Omega' \, \sigma_g \, I = c_g(\theta) \iint_{\hat{\Omega}'_+} I \, d\Omega' + \left(\frac{\partial \sigma_g}{\partial \theta'}\right)_0 \iint_{\hat{\Omega}'_-} \theta' \, I \, d\Omega' + \frac{1}{2}\left(\frac{\partial^2 \sigma_g}{\partial \theta'^2}\right)_0 \iint_{\hat{\Omega}'_-} \theta'^2 \, I \, d\Omega' + \ldots \, . \tag{7}$$

The second term on the right hand side of Eq. (7) is of order $(k_o \ell)^{-1}$ compared with the first, while the third term is of order $(k_o \ell)^{-2}$ compared with the first; these may be neglected in view of assumption (2). Furthermore, since I is so much larger in the forward hemisphere than in the backward hemisphere we may further approximate

$$\iint_{\hat{\Omega}'_+} I \, d\Omega' \approx \iint_{\hat{\Omega}'} d\Omega' \, I + o\left(\frac{1}{k_o \ell}\right) . \tag{8}$$

Upon using Eqs. (7) and (8) in (6) we obtain

$$\left(\hat{n} \cdot \nabla + \frac{1}{\ell}\right) I(\hat{n}) = \sigma_g(\theta) \iint_{\hat{\Omega}'} d\Omega' \, I(\hat{n}') + \iint_{\hat{\Omega}'_-} d\Omega' \, \sigma_g(\hat{n} - \hat{n}') \, I(\hat{n}') . \tag{9}$$

To simplify the last term in Eq. (9) we recall that for $k_o \ell >> 1$, $\sigma_g(\hat{n} - \hat{n}')$ is sharply peaked about $\hat{n} = \hat{n}'$. Therefore I can be expanded in Taylor series as

$$I(\hat{n}') = I(\hat{n}) + (\hat{n} - \hat{n}') \cdot \nabla_{\hat{n}} I + \frac{(\hat{n} - \hat{n}')^2}{2} \nabla^2_{\hat{n}} I + \ldots . \tag{10}$$

Upon using Eq. (10) in (9) we obtain

$$\hat{n} \cdot \nabla I + \frac{1}{\ell_a} I - \left(\frac{\Sigma^2}{4\ell_t}\right) \nabla^2_{\hat{n}} I = \sigma_g(\theta) \iint_{\hat{\Omega}'} d\Omega' \, I(\hat{n}') , \tag{11}$$

where

$$\frac{\Sigma^2}{\ell_t} = 2\pi \int_0^\infty n^3 \, \sigma_g(n) \, dn .$$

We must next calculate $\iint I(\hat{n}')\, d\Omega'$. This can be done by multiplying Eq. (1) by $d\Omega$ and integrating over all solid angle. Upon using the fact that $\ell_t^{-1} = \iint \sigma_g\, d\Omega$, we obtain

$$\iint (\hat{n} \cdot \nabla I)\, d\Omega + \frac{1}{\ell_a} \iint I\, d\Omega = 0. \tag{12}$$

For a plasma stratified only in the z-direction Eq. (12) becomes

$$\frac{d}{dz} \iint I\, d\Omega + \frac{1}{\ell_a} \iint I\, d\Omega = 0 \tag{13}$$

which has a solution

$$\iint I\, d\Omega = I(z=0)\, \exp\left\{ - \int_0^z \frac{dz'}{\ell_a} \right\}. \tag{14}$$

Eq. (14) is also approximately correct, even if the plasma is also weakly stratified in the x and y directions. We then have

$$\iint \hat{n} \cdot \nabla I\, d\Omega = \iint n_x \frac{\partial I}{\partial x}\, d\Omega + \iint n_y \frac{\partial I}{\partial y}\, d\Omega + \iint n_z \frac{\partial I}{\partial z}\, d\Omega$$

$$= \frac{\partial}{\partial x} \int_0^{\pi} \int_0^{2\pi} \sin^2\theta \cos\phi\, I\, d\theta\, d\phi + \frac{\partial}{\partial y} \int_0^{2\pi} d\phi \int_0^{\pi} d\theta \sin^2\theta \sin\phi\, I$$

$$+ \frac{\partial}{\partial z} \int_0^{2\pi} d\phi \int_0^{\pi} d\theta \sin\theta \cos\theta\, I. \tag{15}$$

Now I is sharply peaked around $\theta = 0$, when $k_0 \ell_a >> 1$. If we define the width of I as θ_0, it is clear that the first two terms are of order $\theta_0^3 \frac{\partial I}{\partial x}$, while the last is of order $\theta_0^2 \frac{\partial I}{\partial z}$. If $\frac{\partial I}{\partial x}$ and $\frac{\partial I}{\partial y}$ are of the same order as $\frac{\partial I}{\partial z}$, then correct to terms of order $\theta_0 << 1$ we can neglect the first two terms in Eq. (15), so that Eqs. (13) and (14) are approximately valid even when there is stratification in the x and y directions.

Using Eq. (14) in (11) finally yields

$$\left(\hat{n} \cdot \nabla + \frac{1}{\ell_a} \right) I - \left(\frac{\bar{\gamma}^2}{4 \ell_t} \right) \nabla_{\hat{n}}^2 I = \sigma_g(\theta) I(z=0)\, e^{-\alpha}, \tag{16}$$

where $\alpha = \int_0^z \frac{dz'}{\ell_a}$. The solution of Eq. (16) will yield an expression for the intensity in the backward hemisphere $\left(\frac{\pi}{2} < \theta \leq \pi\right)$ in the case when $k_o L >> 1$. The third term on the left hand side of Eq. (16) is generally important only when the path length is very large, or θ is near $\pi/2$. To see this let us assume $\ell_t \to \infty$ (no true absorption) and neglect the $\nabla_n^2 I$ term. Then the solution of Eq. (16) for I can be shown to be

$$I(z) = \frac{\sigma_g(\theta)\, I(z=0)}{\cos\theta}\left(z - z_\ell\right),$$

where z_ℓ is the extent of the plasma in the z-direction. Therefore, the ratio of the neglected term in Eq. (13) to those retained is

$$\frac{\frac{\overline{\gamma^2}}{4\ell_t}\nabla_n^2 I}{\sigma_g(\theta)\, I(z=0)} = \frac{1}{4}\left(\frac{z_\ell}{\ell_t}\right)\frac{\overline{\gamma^2}}{\cos^3\theta}. \tag{17}$$

Since $\overline{\gamma^2} << 1$, it requires that either $z_\ell/\ell_t >> 1$ or $\cos\theta << 1$ (or both) for the third term on the left hand side of (16) to be important. Therefore, if $.25\left(z_\ell/\ell_t\right)\left(\overline{\gamma^2}/\cos^3\theta\right) << 1$, we can approximate Eq. (16) by

$$\left(n\cdot\nabla + \frac{1}{\ell_a}\right) I = \sigma_g(\theta)\, I(o)\, e^{-\alpha}. \tag{18}$$

As an example, let us consider the case when the plasma is stratified only in the z-direction, as shown in Figure 2. Equation (18) is then readily solved for I. The result is

$$I(z,\theta) = \frac{I(o)}{\mu}\int_{z_\ell}^{z} dz'\, \sigma_g(z',\theta)\exp\left\{-\int_o^{z'}\frac{dz^*}{\ell_a} - \frac{1}{\mu}\int_{z'}^{z}\frac{dz^*}{\ell_a}\right\} \tag{19}$$

where $\mu = \cos\theta$. The above solution would be useful for obtaining the bistatic RCS for the case when a wake is illuminated by a wave travelling along the wake axis with the receiver located at an angle $\theta_o = \pi - \theta$, where $\theta_o >> 1/k_o L$. Equation (19) does not give the correct intensity when $\theta_o \leq \left(1/k_o L\right)$, for reasons detailed by Watson[5]. When $\theta_o << \left(1/k_o L\right)$, the correct intensity is $I_B = 2I - I_{ss}$, where I is given by Eq. (18), and I_{ss} is the intensity derived in the single scatter approximation and is given by

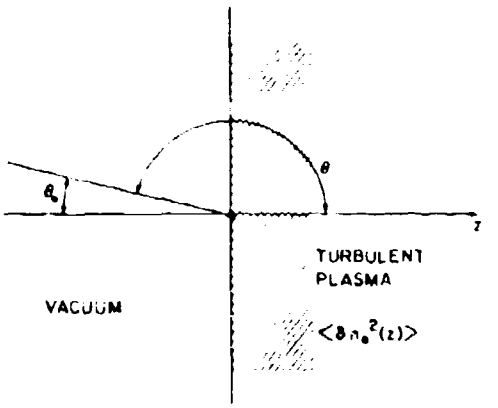

Figure 2. Geometry Assumed in the Derivation of Eqs. (19)-(21)

$$I_{ss} = \frac{I(o)}{\mu} \int_{z_\ell}^{z} \sigma_g(\theta, z') \, e^{-\beta(z')} \, e^{-\frac{1}{\mu}\int_{z'}^{z} \frac{dz''}{\ell}} \, dz' \tag{20}$$

where

$$\beta(z) = \int_0^z \frac{dz'}{\ell} = \int_0^z \frac{dz'}{\ell_a} + \int_0^z \frac{dz'}{\ell_t} .$$

Therefore, in the backscatter cone $\theta_o \ll (k_o L)^{-1}$

$$I = \frac{I(o)}{\mu} \int_{z_\ell}^{z} dz' \, \sigma_g(z', \theta) \exp\left[-\int_0^{z'} \frac{dz''}{\ell_a} - \frac{1}{\mu}\int_{z'}^{z} \frac{dz''}{\ell_a}\right] \left\{1 - \exp\left[-\int_0^{z'} \frac{dz''}{\ell_t} - \frac{1}{\mu}\int_{z'}^{z} \frac{dz''}{\ell_t}\right]\right\} \tag{21}$$

In summary, for the geometry of Figure 2, we use Eq. (21) when $\theta_o \ll (k_o L)^{-1}$ and Eq. (19) for $\theta_o \gg k_o L^{-1}$. When $\theta_o \approx (k_o L)^{-1}$ neither formula is rigorously valid. We note that for $\theta = \pi$ and $\ell_t = \infty$ and z-independence, Eq. (21) reduces to the previous result of deWolf[6,7], that is

6. deWolf, D. (1971) Electromagnetic reflection from extended turbulent medium: simultaneous forward-single-backscatter approximation, IEEE Trans. AP-19: 254-262.

7. deWolf, D. (1972) Discussion of radiative transfer methods applied to electromagnetic reflection from a turbulent plasma, IEEE Trans. AP-20:805-807.

$$I(\theta = \pi) = \sigma_g(\pi)\, I(o)\, z_\ell \left\{ 2 - \frac{\ell_t}{2z_\ell} \left[1 - e^{-\frac{2z_\ell}{\ell_t}} \right] \right\}.$$

3. CALCULATIONS OF BISTATIC RCS

Once the radiative intensity $I(x, \hat{n})$ has been obtained it is quite straightforward to obtain the bistatic (or monostatic) RCS. Consider an element of area dS on the target surface, with the surface normal making an angle ψ with the line joining dS to the receiver, as shown in Figure 3. Let $I(S, \hat{n})$ be the scattered intensity crossing dS in the direction of $\hat{n}$ (as we demonstrated in the last section, this quantity satisfies Eq. (13)). Then the received intensity due to dS is

$$dI_r = \frac{dS \cos\psi\, I(\hat{n}, S)}{r^2}$$

where r is the distance from dS to the receiver. The total intensity received from the entire scatterer is

$$I_r = \frac{1}{R^2} \iint dS \cos\psi\, I(\hat{n}, S)$$

where S_o is the surface area of the scatterer, and R is the distance from the center of the scatterer to the receiver. (We can replace r by R, since the receiver is assumed to be in the Fraunhofer zone). Finally, the radar cross section of the scatterer is

$$\sigma = \frac{R^2 I_r}{I(o)} = \frac{1}{I(o)} \iint dS \cos\psi\, I(\hat{n}, S), \qquad (22)$$

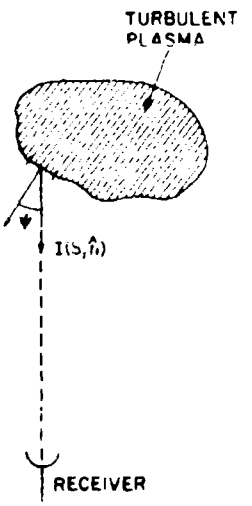

Figure 3. Model Used to Relate the Scattered Intensity to the RCS

4. AN EXAMPLE

As a numerical example let us return to the problem illustrated in Figure 4, and calculate the monostatic and bistatic radar cross section when the rectangular cylinder is illuminated along the z-axis. We will assume that the turbulent eddies in the wake have an exponential correlation function $g(x, r) = \left(<\delta n_e^2> - n_e^2\right) \exp(-r/L)$, where δn_e is the electron density fluctuation. For this case

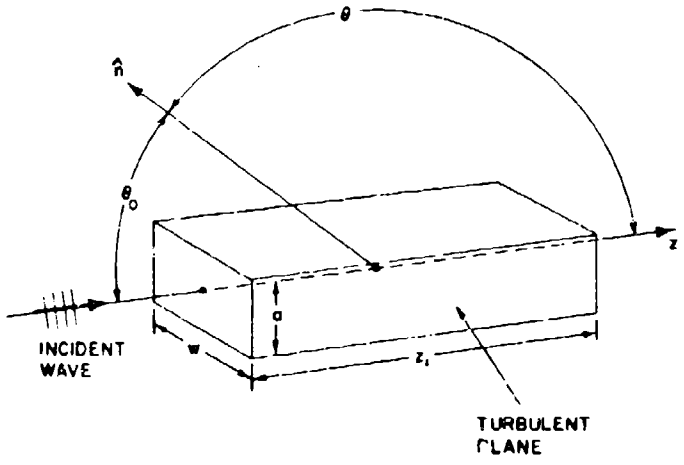

Figure 4. Scattering by a Turbulent Parallelepiped

$$\sigma_g(\theta) = \frac{8\pi r_o^2 L^3 \langle \delta n_e^2 \rangle}{\left(1 + \frac{\nu_c^2}{\omega^2}\right)} \quad \frac{1}{\left[1 + 4(k_1 L)^2 \sin^2(\theta/2)\right]^2} \tag{23}$$

where $k_1 = \rho_1 k_o$ and

$$\frac{1}{\ell_t} = \frac{32\pi^2 \langle \delta n_e^2 \rangle r_o^2 L^3}{\left(1 + \frac{\nu_c^2}{\omega^2}\right)(1 + 4 k_1^2 L^2)} . \tag{24}$$

To simplify the calculation we will assume that $\langle \delta n_e^2 \rangle$ is position independent and that $\nu_c = 0$. We first consider the case when $\theta_o \equiv \pi - \theta \gg 1/k_o L$. Here the scattered intensity satisfies Eq. (18) with $\ell_s \to \infty$. Upon using the solution of Eq. (18) in (22) we find that the contribution to the cross section from the top face of the rectangular cylinder is $\sigma_{top} = \sigma_g(\pi - \theta_o) \tan|\theta_o| z_1^2 w/2$, while the contribution from the front face is $\left(z_1 wa - (z_1^2/2) w \tan|\theta_o|\right) \sigma_g(\pi - \theta_o)$ so that the net bistatic cross section is

$$\begin{aligned} \sigma &= \sigma_g(\pi - \theta_o) z_1 wa \\ &= \sigma_g(\pi - \theta_o) V \end{aligned} \tag{25}$$

where V is the total volume of the plasma. Therefore, for $\pi/2 > \theta_o >> 1/k_o L_o$ the rigorous result agrees identically with the result one would obtain from the first Born approximation.

When $\theta_o = \pi - \theta << (k_o L)^{-1}$, the scattered intensity is given by Eq. (21). Upon applying Eqs. (21) and (22) to the illuminated faces of the rectangular cylinder we find that the net radar cross section of the plasma is (for $|\zeta_o| << (k_o L)^{-1}$)

$$\sigma = \sigma_g (\pi - \theta_o) V \left[2 - \frac{(1 - e^{-2\tau})}{2\tau} - \frac{|\zeta_o|}{\tau} \left(\frac{\ell_t}{a} \right) \left\{ \frac{1}{2} + \left(\frac{3}{2} + \tau \right) e^{-2\tau} - 2 e^{-\tau} \right\} \right] \qquad (26)$$

where $\tau = z_1/\ell_t$. In the limit when $|\theta_o| = 0$, this result reduces to the previous result obtained by de Wolf. The results of Eqs. (25) and (26) can readily be generalized to the case when $< \delta n_e^2 >$ and ν_c depend on z. In that case we have from Eqs. (21) and (22) that the backscatter cross section is

$$\sigma_{back} = \frac{V}{z_1} \int_{z_i}^{0} dz' \, \sigma_g (\pi, z') \exp \left[-2 \int_o^{z'} \frac{dz''}{\ell_a} \right] \left\{ 2 - \exp \left[-2 \int_o^{z'} \frac{dz''}{\ell_t} \right] \right\} \qquad (27)$$

where ℓ_a is given by Eq. (3), ℓ_t is given (24), and $\sigma_g (z', \theta)$ is given by Eq. (23).

We note, again, that for $\theta_o \sim (k_o L)^{-1}$ neither Eq. (25) nor (26) is strictly valid, and the actual solution in that regime is a smooth transition between these two solutions.

5. CONCLUSIONS

We have found that for underdense turbulent plasmas in which the scale size of the turbulent eddies is larger than the signal wavelength, the following is true:

(a) The first Born approximation gives the exact bistatic cross-section, provided $\theta_o >> (k_o L)^{-1}$ and θ_o is not so close to $\pi/2$ that the inequality $.25 \overline{\gamma^2} (z_1/\ell_t) |\cos^{-3} \theta_o| << 1$ is violated.

(b) For θ_o very near zero the backscatter RCS is given by Eq. (27). We note that for this case, whenever $z_1/\ell_t >> 1$ both the Born approximation[1-3] and the modified Born approximation[4] are incorrect.

(c) For values of θ_o of order $1/k_o L$ neither the Born approximation nor Eq. (27) is strictly valid, and the solution there is a smooth transition between the solution for $\theta_o << (k_o L_o)^{-1}$ and for $\theta_o >> (k_o L_o)^{-1}$.

References

1. Booker, H. (1959) Radio scattering in the lower ionosphere, J. Geophys. Res. 64:2164-2177.
2. Salpeter, E., and Trieman, S. (1964) Backscatter of electromagnetic radiation from turbulent plasma, J. Geophys. Res. 69:869-881.
3. Luzzi, T. E. (1969) EM scattering from a finite volume turbulent plasma, IEEE Trans. Antenna & Propagation AP-17:342-348.
4. Graf, K. A., and Guthart, H. (1971) Application of a simple model for calculating scatter, Phys. Fluids 14:410-413.
5. Watson, K. M. (1969) Multiple scattering of electromagnetic waves in a dense plasma, J. Math. Phys. 10:688-702.
6. deWolf, D. (1971) Electromagnetic reflection from extended turbulent medium; simulative forward-single-backscatter approximation, IEEE Trans. AP-19: 254-262.
7. deWolf, D. (1972) Discussion of radiative transfer methods applied to electromagnetic reflection from a turbulent plasma, IEEE Trans. AP-20:805-807.